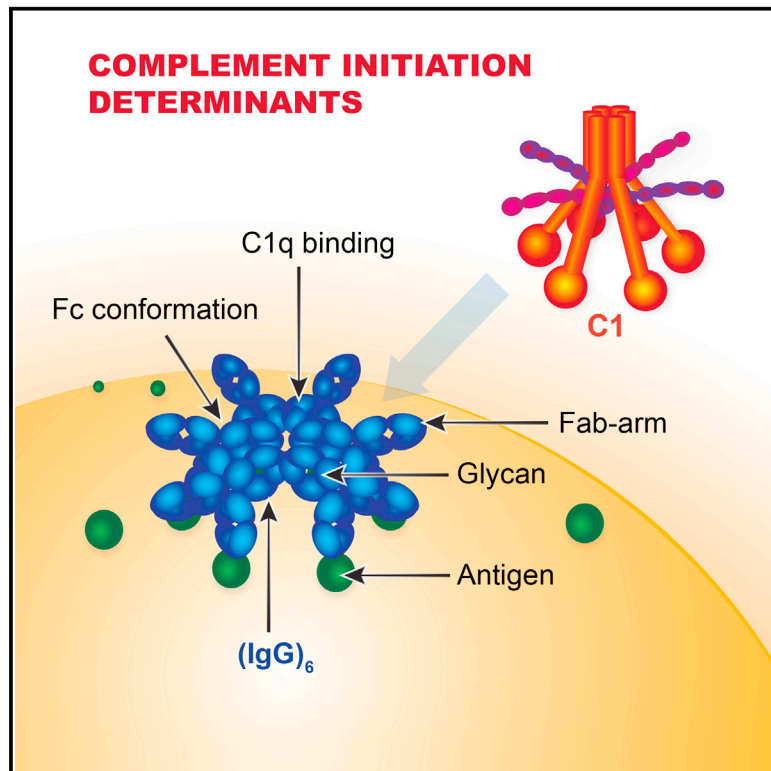# Molecular Basis of Assembly and Activation of Complement Component C1 in Complex with Immunoglobulin G1 and Antigen

Graphical Abstract

Authors

Guanbo Wang, Rob N. de Jong, Ewald T.J. van den Bremer, ..., Janine Schuurman, Paul W.H.I. Parren, Albert J.R. Heck

Correspondence

p.parren@genmab.com (P.W.H.I.P.), a.j.r.heck@uu.nl (A.J.R.H.)

In Brief

Through certain mutations, Wang et al. stabilize IgG hexamers and demonstrate, by native mass spectrometry, how they bind efficiently to C1q/C1. Molecular features of these IgG hexamers, such as glycosylation, are assessed for their specific role in complement activation.

Highlights

- Complement components C1q and C1 bind efficiently to soluble IgG hexamers

- IgG glycosylation contributes to both the hexamer stability and C1q binding

- A complement initiation complex is reconstituted and visualized by mass spectrometry

CrossMark

CellPress

CellPress

Molecular Basis of Assembly and Activation of Complement Component C1 in Complex with Immunoglobulin G1 and Antigen

Guanbo Wang,[1,2,6] Rob N. de Jong,[3,6] Ewald T.J. van den Bremer,[3] Frank J. Beurskens,[3] Aran F. Labrijn,[3] Deniz Ugurlar,[4] Piet Gros,[4] Janine Schuurman,[3] Paul W.H.I. Parren,[3,5,7,*] and Albert J.R. Heck[1,2,7,*]
[1]Biomolecular Mass Spectrometry and Proteomics, Bijvoet Center for Biomolecular Research and Utrecht Institute for Pharmaceutical Sciences, Utrecht University, Padualaan 8, 3584 CH Utrecht, the Netherlands
[2]Netherlands Proteomics Centre, Padualaan 8, 3584 CH Utrecht, the Netherlands
[3]Genmab, Yalelaan 60, 3584 CM Utrecht, the Netherlands
[4]Crystal and Structural Chemistry, Bijvoet Center for Biomolecular Research and Department of Chemistry, Faculty of Science, Utrecht University, 3584 CH Utrecht, the Netherlands
[5]Department of Immunohematology and Blood Transfusion, University Medical Center, Albinusdreef 2, 2333 ZA Leiden, the Netherlands
[6]Co-first author
[7]Co-senior author
*Correspondence: p.parren@genmab.com (P.W.H.I.P.), a.j.r.heck@uu.nl (A.J.R.H.)
http://dx.doi.org/10.1016/j.molcel.2016.05.016

SUMMARY

The classical complement pathway contributes to the natural immune defense against pathogens and tumors. IgG antibodies can assemble at the cell surface into hexamers via Fc:Fc interactions, which recruit complement component C1q and induce complement activation. Biophysical characterization of the C1:IgG complex has remained elusive primarily due to the low affinity of IgG-C1q binding. Using IgG variants that dynamically form hexamers efficient in C1q binding and complement activation, we could assess C1q binding in solution by native mass spectrometry and size-exclusion chromatography. Fc-domain deglycosylation, described to abrogate complement activation, affected IgG hexamerization and C1q binding. Strikingly, antigen binding by IgG hexamers or deletion of the Fab arms substantially potentiated complement initiation, suggesting that Fab-mediated effects impact downstream Fc-mediated events. Finally, we characterized a reconstituted 2,045.3 ± 0.4-kDa complex of intact C1 bound to antigen-saturated IgG hexamer by native mass spectrometry, providing a clear visualization of a complete complement initiation complex.

INTRODUCTION

As a potent defense cascade of innate immunity, the complement system contributes to the natural immune response against pathogens and tumors (Ehrnthaller et al., 2011). The antibody (Ab)-dependent classical pathway of complement activation is triggered when C1q, the IgG recognition component of the C1 complex, docks on antigen (Ag)-bound IgM or IgG (Ga-boriaud et al., 2004; Kishore and Reid, 2000). C1q is a complex resembling a bundle of six tulips (Strang et al., 1982), in which one subunit is formed by a trimer of C1q A, B, and C chains, which assemble into a collagen-like stalk connected to a globular headpiece responsible for the recognition of a variety of target patterns (Kojouharova et al., 2010). C1q is composed as a trimer of covalently linked dimeric subunits $A_2B_2C_2$: C1q subchains A and B form a disulfide bridge within an ABC subunit, while a disulfide between two C chains covalently links two ABC subunits. C1q associates with the proteases C1r and C1s, which are activated by C1q target binding (Gaboriaud et al., 2014). Mass spectrometry (MS) characterization of C1q subunits demonstrated their complex post-translational modification, and it enabled identification of amino acids crucial to protein-protein interactions (Pflieger et al., 2010; Petillot et al., 1995; Brier et al., 2010).

Only in the form of oligomers, IgG is endowed with sufficient C1q-binding avidity to activate complement (Hughes-Jones and Gardner, 1979; Sledge and Bing, 1973; Burton, 1990). The instability of the C1q-Ab complex in solution also has complicated the detailed biophysical and functional characterization of this initiation step in the classical complement pathway upon reconstitution from purified components. As a consequence, the molecular events underlying the mechanism of C1 activation by IgG have remained elusive, and the role of molecular determinants, such as glycan form and Ag binding, has been inferred predominantly from functional activity or studied using isolated Ab fragments.

Recently, we reported that complement is activated efficiently by IgG hexamers assembled at the cell surface through Fc:Fc interactions (Diebolder et al., 2014), addressing the functional relevance of oligomeric IgG structures previously observed under several non-physiological conditions (Burton, 1990; Kuznetsov et al., 2000; Pinteric et al., 1971). We identified a number of specific single-point mutations in the IgG1 Fc domain that stimulated hexamerization and complement activity of the mutated Ab after its binding to cell surface-expressed Ag (de Jong
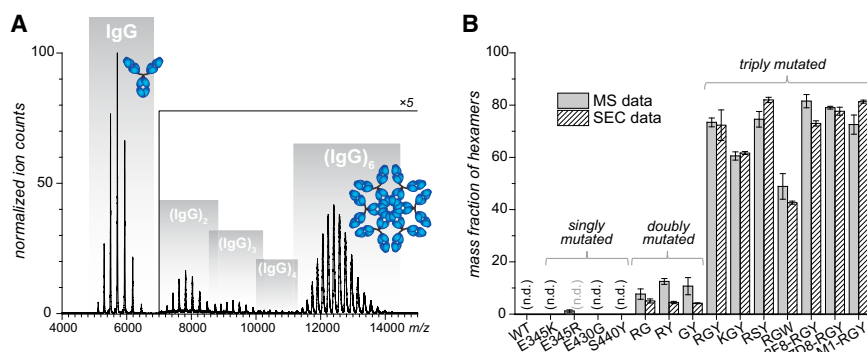
CrossMark

Figure 1. Measurements of Hexamerization Propensity of IgG Mutants in Solution by Native MS and SEC Are Highly Consistent

(A) Different oligomeric states of IgG1-005-RGY (indicated in subscripts) could be identified by native MS. Intensities of the signals with m/z higher than 7,000 were magnified 5× for better visualization of these oligomers. Schematic structures of the IgG monomer and hexamer are shown beside the corresponding peaks.

(B) Fractional masses of IgG incorporated in the hexameric state (%) were determined for the IgG1-005, -2F8, -7D8, and -M1 variants, summarizing data determined by native MS (solid bars) and SEC (striped bars), respectively. Data are presented as average ± SD (n ≥ 3). n.d., non-detectable in both (black) or only SEC (gray) measurements.

See also Figure S1 and Tables S1–S3.

et al., 2016). Interestingly, several such mutations were found to have additive effects, and a variant combining three mutations (i.e., E345R, E430G, and S440Y [RGY]) was shown to readily assemble into hexamers and induce complement activation in solution in the absence of Ag binding (Diebolder et al., 2014).

Here we used a variety of such solution-phase hexamerizing IgG mutants as idealized, high-avidity substrates for C1q binding, which enabled the characterization of C1:IgG complexes by solution-phase biophysical techniques with an emphasis on native MS. This strategy made it possible to shed light on multiple molecular events that underlie the activation of C1 by IgG Abs.

RESULTS

Hexamerization of IgG Ab Leads to Efficient C1q Binding in Solution

To probe the oligomerization propensity of various IgG constructs, we primarily made use of native MS (Heck, 2008; Diebolder et al., 2014; Wang et al., 2012). Native MS offered sufficient resolution and sensitivity to monitor the monomer-hexamer equilibrium of hexamerization-enhanced IgGs, in which individual oligomeric states could be clearly separated and identified (Figure 1A). While monomeric and hexameric $(IgG)_6$ species were the predominating species observed in native mass spectra of the triple mutant IgG1-005-RGY (2 μM), lowly abundant dimer, trimer, and tetramers were detected as well (Figure 1A). The fractional mass of IgG incorporated in the hexameric state was determined for each IgG variant, as an indication of the hexamerization propensity of all tested variants (Figure S1A; see Table S1 for mutations present in all variants and their corresponding abbreviations; see Table S2 for theoretical and measured molecular weight (Mw) values of species analyzed in this work). MS observations were corroborated using ultra-performance liquid chromatography size-exclusion chromatography (UPLC-SEC), in which low-abundant oligomers of intermediate size were detected as a trace slightly above the baseline level between two well-defined peaks corresponding to IgG monomers and hexamers (Figure S1B). These observations suggest a dynamic interconversion between the different oligomeric states.

Summarized in Figure 1B are the fractional masses of hexamers formed by wild-type IgG1-005 and 11 mutated variants (see

also Table S3), which are all able to significantly enhance complement-dependent cytotoxicity (CDC) (Figures S1E and S1F). IgG E345R was the only single mutant that formed detectable hexamers, populating 1% of total mass in the hexameric state. The introduction of additional enhancing mutations dramatically enhanced hexamer propensity, causing an increase in hexameric abundance of the resulting double and triple mutants up to more than 50-fold. The combination of enhancing mutations, exemplified by the 005-RGY triple mutant, induced effective hexamerization regardless of the paratopes of the parental IgG Ab, demonstrated by the hexamerization of RGY variants of Abs 2F8 (anti-EGFR), 7D8 (anti-CD20), and M1 (anti-mannan) (Figure 1B).

The fractional hexamer abundance was quantified from both the native MS and SEC data, and both methods yielded highly consistent results (Figure 1B; Figure S1C). The propensity of IgG hexamerization was found to be concentration dependent. When the concentration of the IgG1-005-RGY was decreased below 2 μM, the hexamer abundance dropped accordingly. At 1 μM IgG concentration, approximately half of IgG1-005-RGY molecules populated the hexameric state.

When C1q was incubated with hexamerization-enhanced IgG variants, stable complexes larger than $(IgG)_6$ or C1q could be observed by SEC (Figure 2A), although with insufficient resolution to determine their exact composition. Native MS analysis of these solutions demonstrated the formation of C1q:IgG complexes predominantly assembled at a stoichiometry of 1:6 (Figure 2B). Although theoretically each IgG molecule contains two identical, symmetry-related C1q-binding sites in its Fc domain, only one copy of C1q was observed to bind per $(IgG)_6$. Under native MS conditions, we also observed the interaction between $(IgG)_6$ and a lower abundant sub-complex of C1q, containing two of the three C1q $A_2B_2C_2$ subunits (Figure 2B; Figures S2A and S2B; Table S4). We could not detect binding of C1q to the minor amounts of IgG dimers, trimers, and tetramers observed. All hexamerization-competent mutants bound C1q in the hexameric state, while C1q:IgG interactions could not be detected for variants incapable of solution-phase hexamerization, indicating IgG hexamerization to be a requirement for C1q binding in this system (Figure S2C). Based on MS signal intensities, we calculated the fractional mass of C1q-bound IgG
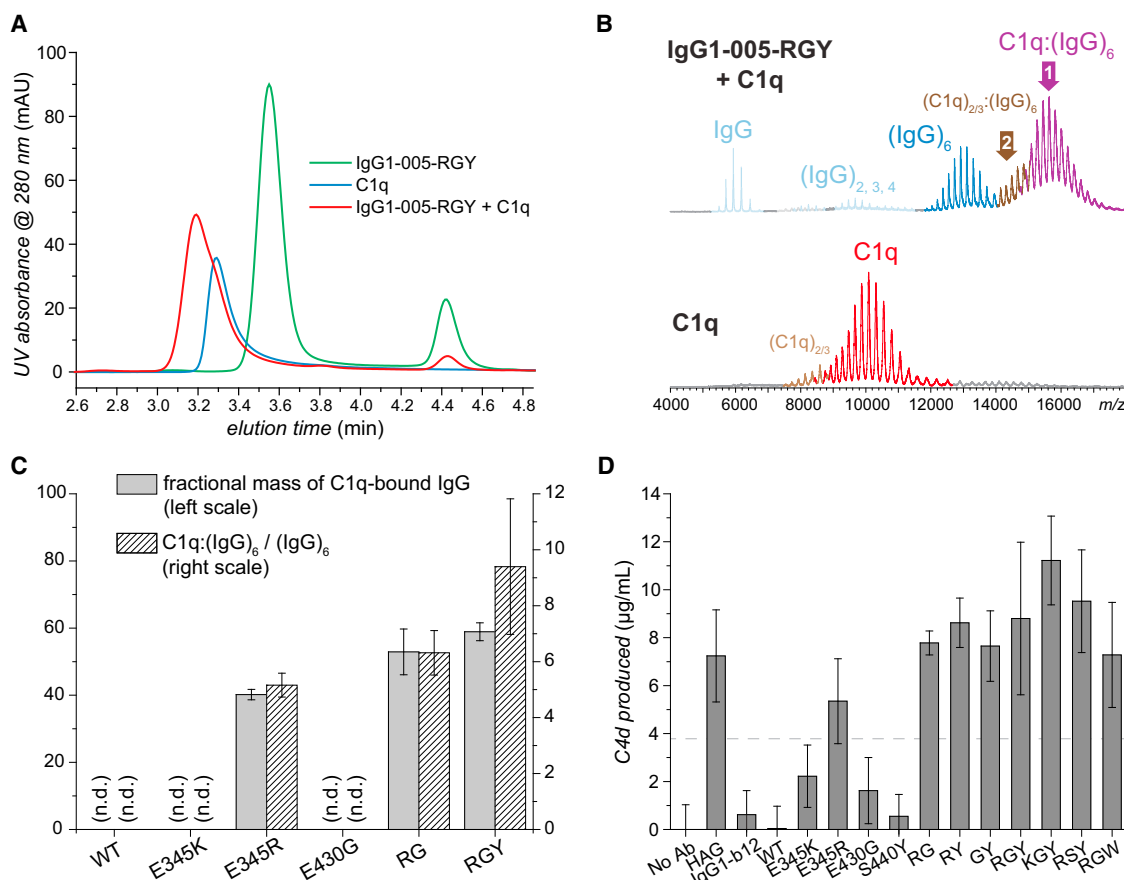
Figure 2. Ab Hexamers Enable Reconstitution of Homogeneous and Functionally Active C1q:IgG$_6$ Complexes

(A) Size-exclusion chromatograms of IgG1-005-RGY and C1q before and after mixing. A higher mass assembly is observed after mixing C1q and IgG-005-RGY.

(B) Accurate mass and binding stoichiometry of C1q:IgG complex determined by native MS. A C1q sub-complex containing two of three A$_2$B$_2$C$_2$ subunits is indicated as (C1q)$_{2/3}$; arrows indicate subpopulations of ions analyzed by tandem MS measurements in Figure S2.

(C) Determination of fractional mass of C1q-bound IgG (%) and equilibrium molar ratio of C1q:(IgG)$_6$ to (IgG)$_6$ for IgG1-005 variants by native MS are shown. n.d., non-detectable.

(D) ELISA measurement of C4d levels generated after incubation of IgG variants in NHS. The baseline is defined as twice the SD of control measurements. Data in (C) and (D) are presented as average ± SD (n ≥ 3). See also Tables S1, S2, and S4.

for several IgG variants to assess the efficiency of C1q binding, and we plotted the equilibrium molar ratios of C1q:(IgG)$_6$ to (IgG)$_6$ to illustrate the apparent C1q-binding affinities of these IgGs (Figure 2C).

To test the functional significance of the observed complexes, hexamerization-enhanced IgGs were incubated with human serum and tested in an ELISA assay capturing soluble C4d, a protein fragment formed as a consequence of C1-mediated proteolysis of complement factor C4 (Figure 2D). All IgG variants displaying efficient solution hexamerization yielded significant production of C4d when incubated in normal human serum (NHS), consistent with their C1q binding observed by native MS and SEC. Even for IgG variants with low-to-modest hexamerization propensity, such as E345R and E345R/E430G (Figure 1B), C1q binding in solution was readily detected (Figure 2C) and corroborated by complement activation (Figure 2D). Efficient C1q binding (Figure S2D) as well as C4d production (Figure S2E) was observed for multiple RGY triple-mutant IgGs directed against

distinct Ags. In summary, all tested IgGs that formed detectable levels of hexamers in solution bound one C1q molecule per IgG hexamer, and they promoted the production of C4d when incubated in human serum.

IgG Glycosylation Contributes to Hexamerization Efficiency and C1q Binding

Changes in glycosylation at residue N297 in the Fc region of human IgG1 and murine IgG2a have been reported to impact complement activity (Tsuchiya et al., 1989; Boyd et al., 1995; Hodoniczky et al., 2005; Leatherbarrow et al., 1985; Duncan and Winter, 1988), and IgG devoid of glycosylation is often used to abrogate classical pathway complement (Lund et al., 1996; Tao and Morrison, 1989). We reasoned that these commonly known defects in complement activation may possibly have been caused by a potential inhibition of IgG hexamerization as an underlying cause that had hitherto gone unnoticed. Therefore, we tested to what extent IgG deglycosylation affects IgG

hexamerization (Figure 3A), C1q binding (Figure 3B), or C1 activation (Figure 3C) by variants with differing hexamerization propensity.

The impact of IgG deglycosylation on hexamer abundance (Figure 3A) varied strongly: the IgG variants with the lowest hexamerization propensity, RG and RGW, displayed a pronounced decrease in hexamer abundance upon deglycosylation. In contrast, deglycosylation of variants RGY and RSY had only a minor impact on their hexamer abundance. Complete deglycosylation was confirmed by MS (Figure S3A). The impact of deglycosylation on the apparent C1q affinity of IgG hexamers was more uniform: all IgG variants for which hexamers could be detected retained their capacity to bind C1q (Figures S3B–S3G), but with reduced apparent affinities compared to their glycosylated counterparts (Figure 3B). Surprisingly, deglycosylation only blocked complement activation in solution by E345R, while the activity of variants with higher hexamer propensity was fully resilient to deglycosylation (Figure 3C).

Fab Arms Contribute to IgG Hexamerization and C1 Activation

In the cryo-electron microscopy (EM) tomography analysis of the membrane-bound IgG molecule (Diebolder et al., 2014), it was observed that one Fab domain was bound to the Ag-coated membrane, while the other Fab domain appeared to reside in the plane of the Fc hexamer. To test whether the non-Ag-bound Fab domain might contribute to IgG hexamer stabilization or complement activation, we generated IgG1-RGY variants lacking either one (Fab1-RGY) or both Fab arms (Fc-RGY). Deletion of one or both Fab arms resulted in a decrease in the fractional mass of IgG present as hexamers by ~30%, but it did not completely abolish hexamerization (Figure 3D). However, both the Fc-only and one-armed IgG variants retained efficient C1q binding (Figure 3E), suggesting that the Fab arms are dispensable for C1q binding. The stoichiometry of these IgG:C1q complexes remained 6:1, consistent with the results obtained with intact IgG, indicating that the inability to bind a second C1q molecule is not caused by the presence of the Fab arms. The removal of Fab arms caused the formation of larger, unspecific aggregates, such as heptamers (7), octamers (8), and dodecamers (12) (Figure S3H), which were not observed with intact IgG. These latter aggregates, however, did not yield detectable C1q binding.

While the Fab arms appeared dispensable for C1q binding, the formed hexamers showed an unexpected potency increase in the activation of C1. Incubating human serum with either Fab1-RGY or Fc-RGY induced a dramatic increase in soluble C4d production (Figure 3F), far exceeding the levels of the RGY and heat-aggregated IgG controls, suggesting that the presence of Fab arms may, to a certain extent, restrict the activation of C1.

Ag Binding by IgG1 Hexamers Contributes to Activation of C1

For regular IgG and IgM Abs, Ag binding is a prerequisite to complement activation (Feinstein et al., 1986; Burton, 1986; Czajkowsky and Shao, 2009). The low affinity of C1q for individual IgG-binding sites restricts C1 activation to surfaces presenting multiple, proximal Ag-bound IgGs to provide a composite C1q-

binding site of sufficient avidity (Diebolder et al., 2014). Our C1q:IgG complexes assembled in solution provided a unique opportunity to assess whether the binding of monovalent Ags might directly contribute to IgG hexamerization, C1q binding, and complement activation. We used the extracellular domain of CD38 (CD38-ECD) as a model Ag that is strongly bound (nanomolar affinity) to the IgG1-005 Ab and Fc variants used.

When CD38-ECD was titrated into a solution containing IgG1-005-RGY, the maximal Ag-binding capacities of IgG monomers and hexamers were determined to be 2 and 12, respectively. The Mw for the latter complex could be determined by native MS to be 1,255.2 ± 0.1 kDa. These findings are consistent with complete occupancy of both Fab-Ag-binding sites in each individual IgG molecule (Dyachenko et al., 2015) (Figure S4A). We observed little cooperativity in Ag recruitment, as the number of Ags incorporated into the IgG-Ag complexes increased evenly throughout the titration without any sharp transition. While the capacity of Ag accommodation was not compromised by IgG hexamerization, Ag binding in turn did not impact the hexamerization propensity of IgG (Table S3).

To examine whether saturating Ag binding for all Fab domains might affect the recruitment of C1q, we incubated IgG-C1q complexes in the presence of excess Ag. This mixture consisting of C1q, IgG1-005-RGY, and Ag produced a single 1,719.6 ± 0.1-kDa assembly corresponding to a C1q:IgG:Ag complex with a predominant stoichiometry of 1:6:12 (Figure 4A). This stoichiometry was not affected by switching the order of addition of the individual components (i.e., pre-incubating IgG with C1q or IgG with Ag) (Figure S4B). Ag binding did not appear to affect the avidity of IgG hexamers for C1q significantly, as determined by analyzing the equilibrium molar ratios $C1q:(IgG)_6:Ag$ to $(IgG)_6:Ag$ for RG and RGY, in both the presence and absence of Ag (Figure 4B). Surprisingly, the addition of the monovalent CD38-ECD to IgG1-005 hexamers substantially stimulated C4d production after incubation in serum. This stimulation was dependent on specific Ag binding, as the non-specific control Ag CD74-ECD did not affect C4d production by IgG1-005-RGY (Figure 4C). The complement activity of IgG variants that failed to hexamerize in solution was not affected by the presence of Ag. Soluble Ag also failed to further enhance the complement activity of a hexameric IgM variant of IgM-005, produced recombinantly in the absence of the J-chain (Figure 4C). The stimulation of complement activation also was observed for another cognate Ag-binding system: EGFR-ECD binding by anti-EGFR IgG-2F8 variants also promoted the complement activity of formed hexamers (Figure 4D).

Reconstitution and Molecular Visualization of the Complete C1:IgG:Ag Protein Assembly

C1q, consisting of six copies of three different (A, B, and C) chains (Reid, 1979), is the component of C1 responsible for the recognition of cognate Ag (Kishore and Reid, 2000). C1 further encompasses its subunits C1r and C1s that provide catalytic functions, effectively initiating the classical complement pathway (Gaboriaud et al., 2004). The assembly of a $C1:(IgG)_6$ complex was attempted by first reconstituting a C1 sub-complex from purified serum C1q and recombinant C1r and C1s proteins (proenzyme mutants; see the Experimental Procedures for
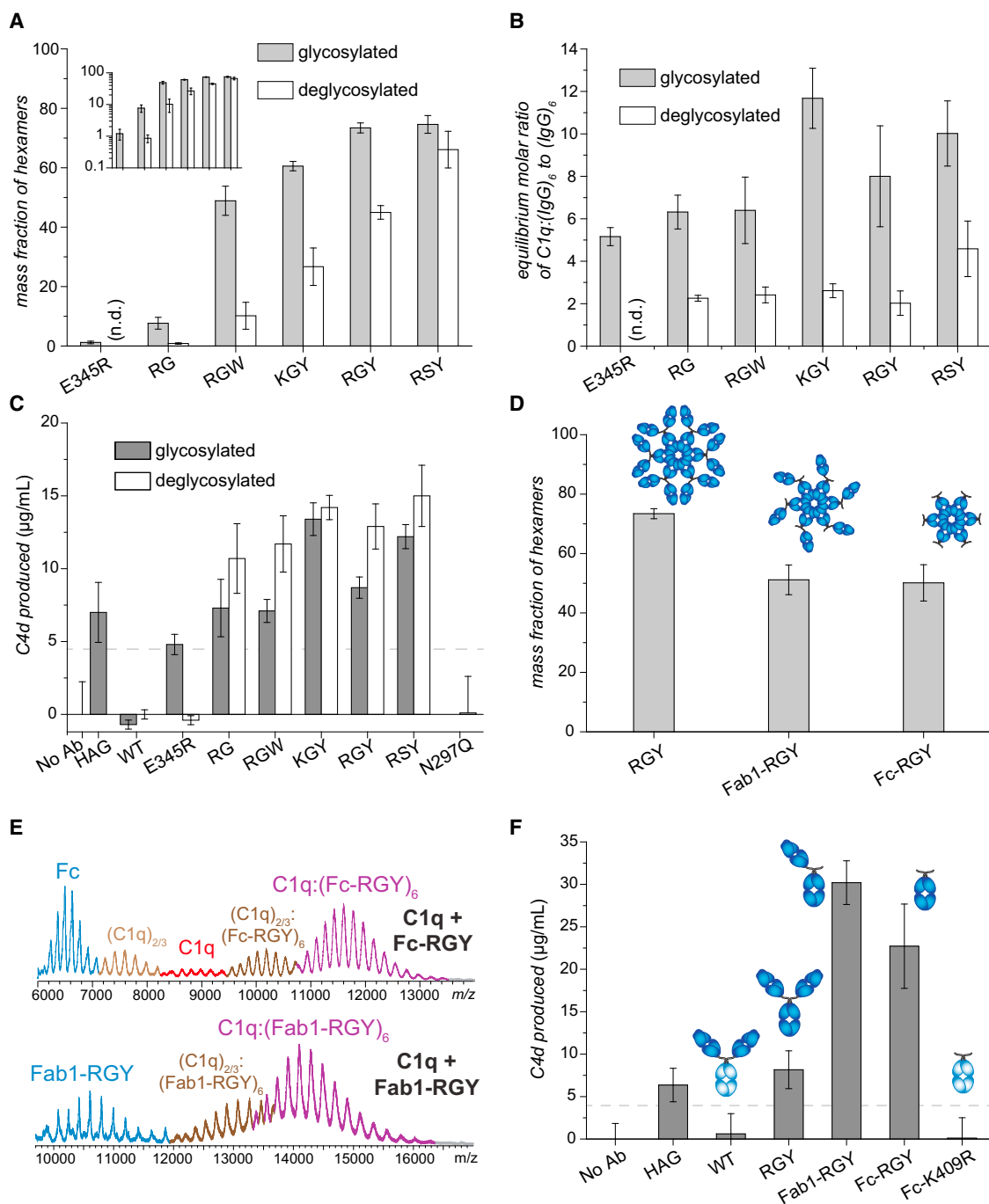
Figure 3. Molecular Determinants Affecting IgG Hexamerization and Complement Activation

(A) Quantification of the impact of deglycosylation on normalized IgG hexamer abundance by native MS, displayed as fractional IgG mass assembled into hexamers (%). The inset stretches the y axis to a logarithmic scale for better visualization of the low levels of hexamerization.

(B) Native MS quantification of the impact of deglycosylation on C1q binding by IgG hexamers is displayed as equilibrium molar ratio of C1q:(IgG)$_6$ to (IgG)$_6$ for several glycosylated and deglycosylated IgG1-005 variants. n.d., non-detectable.

(C) ELISA measurement of C4d generation in NHS induced by glycosylated and deglycosylated IgG1-005 variants is shown.

(D) Native MS quantification of hexamer fractional mass abundance (%) upon deletion of one or both Fab arms in the IgG is shown.

(E) Native mass spectra of C1q incubated with RGY variant hexamers that lack one (Fab1-RGY) or both Fab arms (Fc-RGY). Both species bound efficiently to C1q with the same stoichiometry as intact IgG. (C1q)$_{2/3}$ denotes a C1q sub-complex containing two of three A$_2$B$_2$C$_2$ subunits.

(F) ELISA measurement compares C4d generation in NHS induced by IgG1-005-RGY variants containing two (RGY), one (Fab1), or no Fab arms (Fc-RGY).

Data in (A)–(D) and (F) are presented as average ± SD (n ≥ 3). See also Figure S3 and Tables S1–S4.
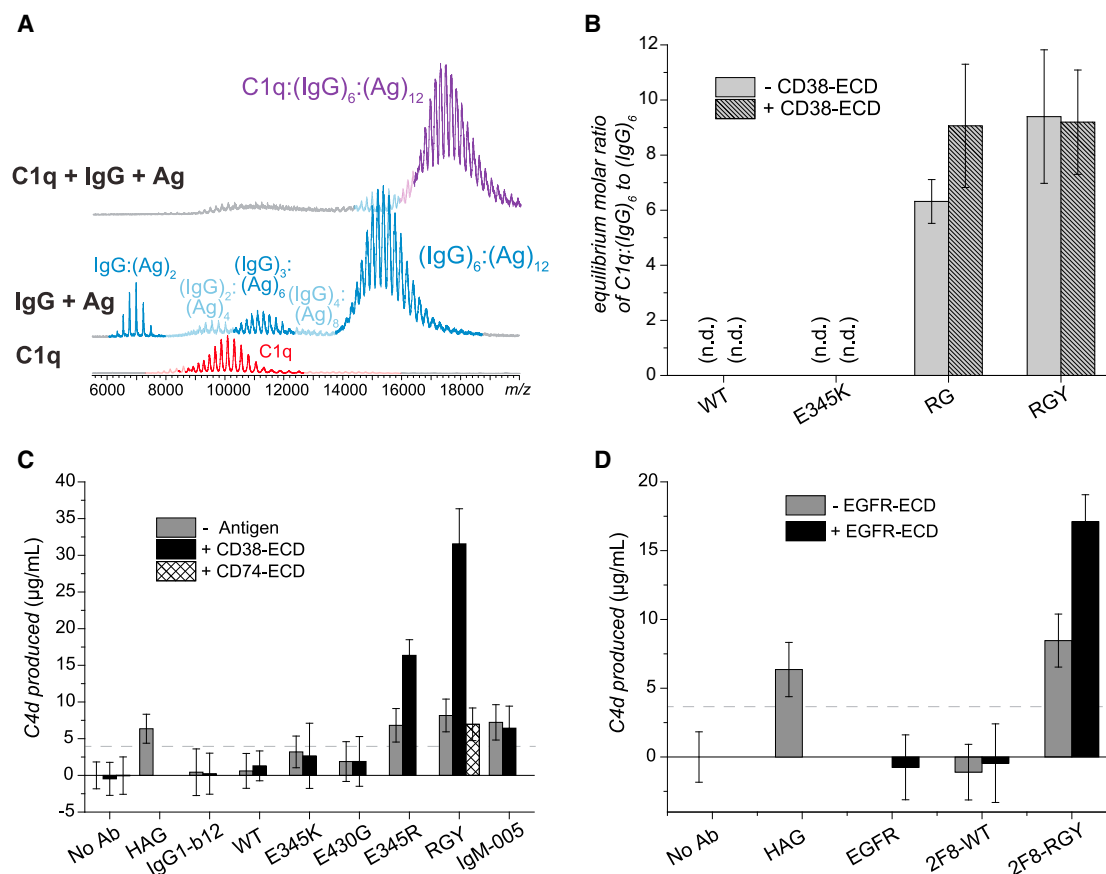
Figure 4. Ag Binding to (IgG)₆ Stimulates Complement Activation
(A) Native mass spectra of Ag- and C1q-binding states of hexameric IgG1-005-RGY show the exclusive formation of a C1q:(IgG)₆:(Ag)₁₂ complex.
(B) Native MS quantitation of C1q binding to Ab hexamers saturated with Ag is displayed as equilibrium molar ratio of C1q:(IgG)₆ to (IgG)₆. n.d., non-detectable.
(C) ELISA measurement of C4d produced after incubation of anti-CD38 Ab IgG1-005 variants in NHS in the presence of cognate Ag CD38-ECD or control Ag CD74-ECD is shown.
(D) ELISA measurement of C4d produced after incubation of anti-EGFR Ab IgG1-2F8 variants in NHS in the presence of cognate Ag EGFR-ECD is shown.
Data in (B)–(D) are presented as average ± SD (n ≥ 3). See also Figure S4 and Tables S1 and S2.

details). The native MS-observed mass of the reconstituted complex containing 22 proteins demonstrated that C1q, C1r, and C1s were assembled at a stoichiometry of 1:2:2 (Figure 5A), in accordance with the reported composition of natural C1 (Cooper, 1985; Arlaud et al., 1987; Brier et al., 2010). The reconstituted C1 was able to bind effectively to the IgG1-005-RGY hexamer, exhibiting the same binding stoichiometry as C1q (Figure 5A).

In the presence of excess Ag, the C1:(IgG)₆ complex accommodated maximally 12 copies of Ag (Figure 5A). To unambiguously assign the mass of this complex consisting of 40 protein subunits, a tandem mass measurement was performed (Snijder et al., 2013, 2014), in which intact C1:IgG:Ag complexes were mass-selected inside the mass spectrometer and subjected to collision-induced dissociation (Figure S5). The resulting fragment ions gave rise to better-resolved ion signals (Figure S5), and they enabled confirmation of the predominant C1:IgG:Ag stoichiometry of 1:6:12, with a total mass of 2,045.3 ± 0.4 kDa (Table S2).

DISCUSSION

By using IgG variants containing mutations that facilitate the formation of ordered hexamers in solution (de Jong et al., 2016), we were able to generate C1q-Ab complexes that were sufficiently stable in solution to enable characterization by biophysical and functional methods. Although these variants differ from natural IgG1 at one to three amino acid positions, their functional activity both in solution assays and on cell surfaces supports their relevance to understanding the requirements for Ab-mediated complement activation.

Monomeric IgG is not able to initiate activation of the complement cascade, although its C1q-binding sites are exposed (Feinstein et al., 1986). At the cell surface, the presence of multiple and proximal Ags allows the formation of IgG hexamers that bind C1q with high avidity and that promote efficient complement activation (Diebolder et al., 2014). Specific Fc and C_H2-C_H3 interface mutations were identified that enhance hexamerization and complement activation by IgG (de Jong
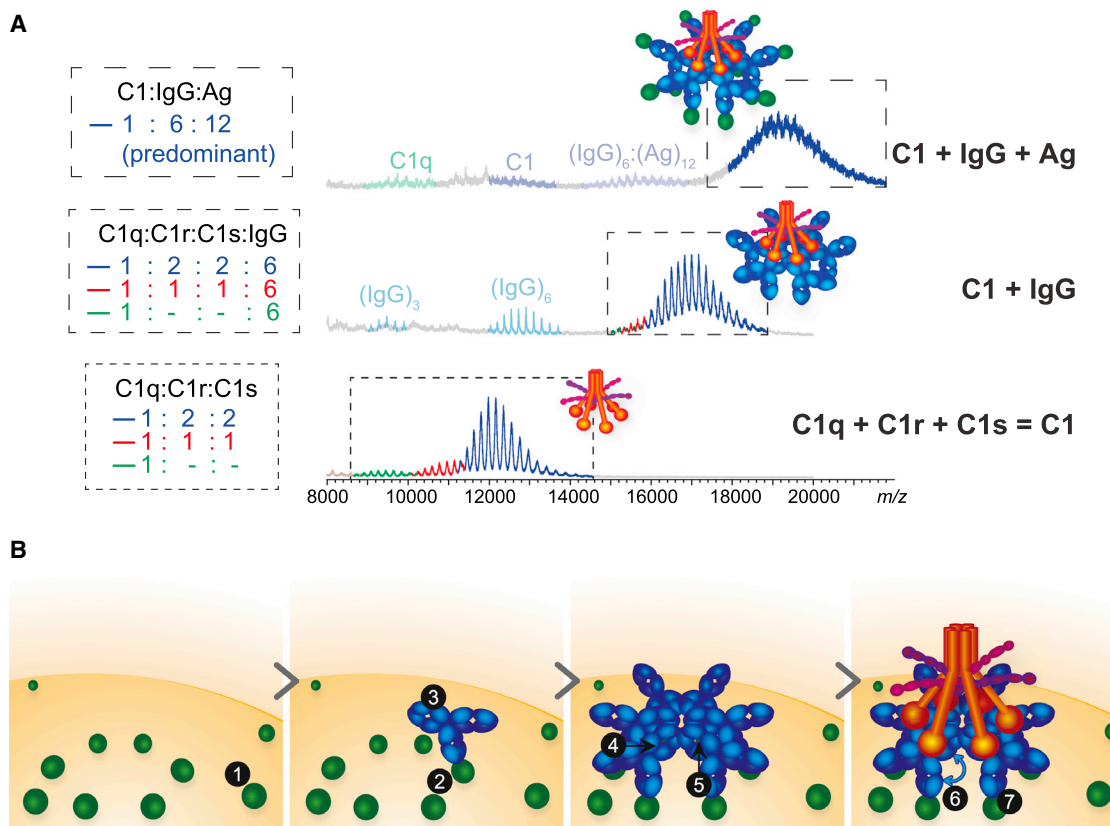
Figure 5. Stepwise Reconstitution of the 2.1-MDa C1:IgG:Ag Complex, Constituting 40 Individual Protein Subunits
(A) Native MS analysis of reconstituted C1, C1:IgG, and C1:IgG:Ag complexes. The signals shown in dashed boxes are color coded according to the stoichiometries of C1 assembling, as specified to the left of the corresponding spectra. The bottom spectrum demonstrates the successful reconstitution of C1, containing next to C1q two copies of C1r and two copies of C1s, although the incomplete version was present in low abundance; the middle spectrum shows that the latter assembly successfully binds to $(IgG)_6$ and subsequently to 12 copies of Ag. See also Figure S5 and Tables S2 and S4.
(B) Model summarizing molecular determinants contributing to IgG-mediated activation of the classical complement pathway. The assembly of the complement initiation complex is proposed to be dependent on (1) the availability of specific antigens recognized by IgG Abs, (2) Ag compatibility with clustering at the cell surface or in solution, (3) the Fc-domain conformation, (4) the high-avidity binding site for hexavalent C1q, (5) the composition of the IgG glycan chains, (6) the presence of Fab arms, and (7) antigen binding by Fab arms.

et al., 2016). A triple combination of these mutations was shown to mediate the formation of ordered hexameric IgG ring structures in solution in the absence of Ag, suggesting that they may represent a conformation optimal to C1q binding (Diebolder et al., 2014).

Interestingly, also IgG variants forming hexamers in solution at low abundance, such as E345R, bound C1q and induced complement activation in solution (Figure 2; Figure S4A). It appears that mutual stabilization between the multivalent C1q and IgG hexamer may drive their binding equilibrium from threshold levels of free IgG hexamer toward the complexed state. Only Abs detectably hexamerizing in solution could bind C1q or activate complement in solution efficiently, as illustrated by control Abs and variants E430G and E345K (Figures 2C and 2D). Combined with the observation that the described CDC-stimulating single mutations (de Jong et al., 2016) all promoted increased hexamerization in solution when combined into double or triple mutants (Figure 1), this suggests that IgG hexamerization is prerequisite to C1q binding and C1 activation.

The possible role of the Fc-domain conformation in IgG hexamerization and C1q recruitment was assessed by using mutated and deglycosylated IgG. Mutation E430G may allosterically affect the formation and stability of hexameric IgG (de Jong et al., 2016). Amino acid E430 participates in a salt bridge that stabilizes the C_H2-C_H3 interface packing (Saphire et al., 2001) (IgG fold nomenclature according to Halaby et al., 1999) and could inhibit Fc:Fc interactions by restraining Fc flexibility. Even conservative and charge-preserving mutations of this residue dramatically enhanced CDC (de Jong et al., 2016). When mutation E430G was introduced into variants S440Y or E345R, it enhanced their hexamerization propensity (Figure 1B) and serum C4d production (Figure 2D). IgG variants containing E430G or E430S displayed increased C1q-binding capability (Figure 2C) and CDC potency (Figure S2), highlighting the role of Fc-domain flexibility in efficient IgG hexamerization and subsequent C1 activation.

The importance of Fc-domain conformation to both IgG hexamerization and subsequent complement activation was

emphasized by removal of the glycan chain connected to N297 in the IgG heavy-chain C_H2 domain (Figure 3). Each bi-antennary oligosaccharide chain extends one arm toward the C_H2-C_H3 interface region and the other arm into the space between the C_H2 domains, making multiple interactions with the surface of the C_H2 domain and the glycan of the opposing C_H2 domain, respectively (Krapp et al., 2003), resulting in a horseshoe-like Fc-domain conformation. Glycosylation stabilizes the C_H2 domain, while the truncation of N-linked glycan sugar moieties leads to conformational changes, a decrease in thermal stability, and loss of effector functions (Jefferis, 2012). Optimal C1 activation appeared to require, or be sensitive to, certain defined oligosaccharide structures, especially terminal sugar residues, in the glycan chain attached to IgG, with C1q-mediated effector functions being compromised or ablated for aglycosylated or deglycosylated IgGs (Jefferis, 2012). Complement activity can be modulated by remodeling of the IgG glycan chain using the endoglycosidase EndoS; potential clinical applications have been studied in experimental animal models of, for example, autoimmune hemolysis and glomerulonephritis (Allhorn et al., 2010; Yang et al., 2010; Goodfellow et al., 2012).

In Figure 3, we tested if complement inhibition by deglycosylation may be partially attributed to inhibition of IgG hexamerization. IgG hexamerization was inhibited by deglycosylation most strongly for IgG variants displaying the lowest hexamer abundance (Figure 3A). C1q binding also was reduced by deglycosylation for all detectable IgG variant hexamers, but to relatively comparable efficiency (Figure 3B). All variants retaining detectable hexamer abundance remained capable of activating complement in solution at surprising efficiency (Figure 3C), while deglycosylated E345R without detectable hexamer abundance lost this activity completely. We conclude that IgG deglycosylation may unexpectedly have a pronounced effect on C1q-binding avidity via modulation of IgG Fc:Fc interactions, rather than the commonly considered possible reduction of C1q-binding affinity (e.g., through local structural changes). It appears that, in the hexameric state, mutual Fc:Fc interactions and C1q binding help to lock Fc domains in a complement activation-competent state.

IgG hexamers appear to be stabilized by their Fab domains, as hexamer abundance decreased moderately upon removal of one or both of the Fab arms (Figure 3D). Surprisingly, removal of either a single or both Fab arms significantly improved the complement activity of the tested Abs (Figure 3F), which suggests that Fab arms may have a regulatory role during activation of C1. In our cryo-EM tomography study of C1 bound to hexameric IgG, the non-Ag-bound Fab arms appeared to reside in the plane of the Fc hexamer, in close proximity to the C1q head-pieces (Diebolder et al., 2014). Intriguingly, a possible regulatory role of IgG Fab arms also was suggested by the stimulation of complement activation by Ag binding to hexameric IgG (Figure 4). While Ag binding had little impact on the C1q-binding avidity of IgG hexamers formed in solution (Figure 4B), binding of two different cognate Ags to two different Abs promoted their complement activity (Figures 4C and 4D). We speculate that this activation may be caused by conformational changes in the C1q:IgG complex induced upon Ag accommodation in the IgG, suggesting a conformational signal is conveyed from the Ag-bound Fab arm into the Fc domain.

Combining our observations with the results from prior studies of complement activation at the cell surface (Diebolder et al., 2014; Feinstein et al., 1986), we propose a model of molecular IgG determinants affecting classical pathway complement activation by IgG in Figure 5B. The assembly of the complement initiation complex is dependent on (1) the availability of specific Ags recognized by IgG Abs. Only some epitopes on a limited number of Ags induce complement activation when bound by (monoclonal) IgG1. (2) Possibly, compatibility with surface or solution Ag clustering is prerequisite to the formation of IgG complexes, which also is affected by (3) the Fc-domain conformation imposed by Fc glycan chains or Fc-domain mutations such as E430G, as well as by post-translational processing of the C-terminal lysine (van den Bremer et al., 2015). Hexameric IgG complexes provide (4) a high-avidity binding site for hexavalent C1q, the recruitment of which is sensitive to (5) the composition of the IgG glycan chains. Activation of C1 appears to be modulated both by (6) the presence of Fab arms and by (7) Ag binding by Fab arms, which may, for example, induce IgG or C1 conformational changes, or optimal recruitment or processing of the C1 substrate C4.

By examining the formation of IgG hexamers and the assembly of the macromolecular complex of Ag, Ab; and C1q, C1r, and C1s, we provided insight into the molecular determinants that govern complement activation. It is intriguing that maximal complement activation by IgG may be fine-tuned by such diverse molecular determinants as its glycosylation state, C-terminal lysine processing (van den Bremer et al., 2015), the Fc conformation required for hexamerization providing the binding avidity to interact with C1q, and the conformation and Ag-binding state of the Fab arms.

EXPERIMENTAL PROCEDURES

Proteins and Chemicals
All Abs, Ags, and complement factor mutants C1r-S654A and C1s-S632A were recombinantly expressed and purified in-house as described subsequently. Purified natural human C1q was purchased from Complement Technology. All other chemicals were of analytical grade or higher.

Construction, Expression, and Purification of Recombinant Proteins
Abs were expressed using an IgG1 heavy chain with the human allotype G1m(f). The following monoclonal Abs were used: CD20 monoclonal antibody (mAb) IgG1-7D8 (Teeling et al., 2004), CD38 mAb IgG1-005 (de Weers et al., 2011), EGFR mAb IgG1-2F8 (Bleeker et al., 2004), HIV-1 gp120 mAb IgG1-b12 (Burton et al., 1994), and anti-mannan mAb IgG1-M1 (Zhang et al., 2006). Detailed procedures were described previously (de Jong et al., 2016). Briefly, Ab variants containing the mutations in the IgG1 heavy-chain constant region specified in Table S1 were generated by gene synthesis (Geneart) and cloned into a pcDNA3.3 expression vector (Life Technologies) or by primer-directed site-specific mutagenesis on the expression vector and verified by DNA sequencing. Abs were expressed in HEK293F cells or EXPI293 cells (Life Technologies) by transient transfection according to the instructions supplied by the manufacturer. The fraction of intact Abs at capillary electrophoresis (CE)-SDS exceeded 90%, and the fraction of HC + LC exceeded 95%. A high performance (HP)-SEC release criterion was not applied, since many variants were selected or designed to specifically hexamerize in solution, as described in Figure 1 and Figure S1.

Variant Fc-RGY is a recombinantly expressed Fc domain, spanning amino acids (aa) 266–447 (CPPC…SPGK) of human IgG1 m(f). Fab1-RGY containing a single Fab arm was created by controlled Fab-arm exchange between molecules Fc-E345R/F405L/E430G/S440Y and IgG1-E345R/K409R/E430G/S440Y,

essentially as described previously (Labrijn et al., 2014). Exchange of the Fab arms was confirmed by non-reducing CE-SDS and yielded 87% heterodimer; the remaining homodimeric IgG1 and Fc were determined at 4% and 2% of total protein, respectively. The heavy chain of IgM-005 was generated by gene synthesis of the IgG1-005 heavy-chain variable domain fused to human IgM (CAA34971). The protein was produced by cotransfecting an IgG1-005 Kappa light-chain vector with an IgM-005 heavy-chain vector in the absence of J-chain.

A codon-optimized construct was generated for the recombinant expression of soluble His-tagged CD38 extracellular domain by gene synthesis (Geneart). CD38 aa 45–300 (GenBank: AAA68482) was expressed with an N-terminal His-tag containing six His residues (CD38-ECDHis). The gene fragment was cloned into pEE13.4 (Lonza Biologics), expressed as described above, and purified from cell supernatant using immobilized metal affinity chromatography. To reduce spectral complexity during MS analysis, a variant was generated by gene synthesis (Geneart) in which four asparagine aa at positions 100, 164, 209, and 219 modified by N-linked glycosylation in the natural protein were replaced with aspartic acid, expressed using a pcDNA 3.3 expression vector (Life Technologies).

Soluble extracellular domain of EGFR (EGFR-HisECD) contained aa 25–645 (P00533) fused to a six aa C-terminal His-tag and was produced as described for the CD38 Ags. Soluble extracellular domain of CD74 (CD74-HisECD) contained aa 73–296 (P04233) fused to an N-terminal six aa His-tag and was produced as described for the CD38 Ags. Both proteins were expressed using a pEE13.4 expression vector (Lonza Biologics).

C1r S654A and C1s S632A mutants were generated using the Quikchange mutagenesis kit (Stratagene) on TOPO clones inserted in pCR8 vectors (Invitrogen). Mutant genes were subcloned into mammalian expression vectors provided by U-Protein Express BV (U-PE). C1r S654A (fused to N-terminal His-tag) and C1s S632A (tagless) were co-expressed in N-acetylglucosaminyl-transferase I (GnTI)-deficient HEK293 cells that stably express Epstein-Barr virus nuclear Ag EBNA1 (HEK293-ES). The complex was purified by Ni-NTA affinity chromatography followed by an SEC step on a Superdex 200 column (GE Healthcare).

All protein concentrations were determined by photospectrometry at 280 nm as described previously (de Jong et al., 2016).

Cell Culture and Reagents
Ramos cells (human lymphoma) were obtained from the American Type Culture Collection (ATCC CRL-1596). Cells were cultured in RPMI 1640 supplemented with 10% heat-inactivated CCS, 1 U/ml penicillin, 1 μg/ml streptomycin, and 4 mM L-glutamine. Pooled NHS AB was obtained from Sanquin.

Native MS
All native MS analyses were conducted with a modified LCT time-of-flight (Waters) or hybrid triple-quadrupole/time-of-flight (Waters) mass spectrometer adjusted for optimal performance in high-mass detection. Prior to the analysis, original buffers of recombinant or natural proteins were substituted with a 150-mM ammonium acetate solution (pH adjusted to 7.5 with ammonium hydroxide) through at least five sequential concentration and dilution steps at 4°C using a centrifugal filter with an Mw cutoff of 10 kDa (Merck Millipore). Samples were sprayed from borosilicate glass capillaries mounted to a standard static nanospray source. Tandem MS measurements were performed by mass selection of precursor ions using a quadrupole mass analyzer followed by dissociation of selected ions induced by their collision with xenon molecules in the collision cell. Data analysis was conducted with MassLynx (Waters) and Origin Pro (Origin Lab) software. Relative abundances of oligomeric protein species were determined using a previously described method (Wang et al., 2012). The equilibrium molar ratio of C1q:(IgG)$_6$ to (IgG)$_6$ was calculated by dividing the total intensity of C1q:(IgG)$_6$ signals by the total intensity of (IgG)$_6$ signals detected from solutions containing 2 μM IgG and 0.5 μM C1q. The fractional mass of C1q-bound IgG was determined by dividing the population of IgG incorporated into C1q:(IgG)$_6$ complexes by the total population of IgG, with the concentrations of IgG and C1q increased to 5 and 0.75 μM, respectively, to improve the signal-to-noise ratio in the high m/z region.

Deglycosylation of IgG was performed by incubation with PNGase F (Roche) at 37°C for at least 24 hr. Protein complexes were assembled by mixing the participants at desired ratios followed by incubations at room temperature for at least 10 min (for C1q:IgG and C1 complexes) or 30 min (for C1q:IgG:Ag, C1:IgG, and C1:IgG:Ag complexes) in each step. Calcium acetate (20 μM) was added to stabilize the reconstituted C1 complex.

CDC Assay
CDC assays were performed as described (Pawluczkowycz et al., 2009) with an Ab concentration series diluted in PBS (pH 7.4) (B Braun) and NHS (20% final concentration) as a source of complement. Killing was calculated as the fraction (%) of propidium iodide staining-positive cells determined by a BD FACSCanto II flow cytometer for Ramos B cells.

Complement Activation in NHS
Complement activation was determined by measuring C4d concentrations, a marker for classical complement pathway activation, after incubating 100 μg Ab in 90% NHS for 1 hr at 37°C. C4d concentrations were measured in an ELISA (MicroVue C4d EIA kit, Quidel) generally according to the manufacturer's instructions, with the exception that all C4d levels were determined using 1:100 diluted samples in order to circumvent non-linearity deviations introduced by comparing different dilutions. Deglycosylation of IgG for complement assays was performed by incubation with PNGase F (Prozyme) at 37°C for at least 24 hr. The enzyme was removed by Protein A purification of the IgG using Protein A HP SpinTrap columns (GE Healthcare) according to the instructions supplied by the manufacturer. The extracellular domains of Ags CD38, CD74, and EGFR were incubated with 0.7 μM Ab solutions where indicated at sub-saturating concentrations of 0.7, 0.8, and 0.3 μM, respectively. Full deglycosylation was confirmed by non-native MS.

UPLC-SEC Analysis
SEC analysis was performed using a UPLC Acquity H-class system (Waters) connected to an Acquity UPLC BEH450 SEC 2.5-μm, 4.6 × 150-mm column. Samples were injected (5 μl) containing 1,000 μg/ml total protein and were separated at 0.3 ml/min in 10 min in 0.1 M Na$_2$SO$_4$ buffered at pH 6.8. Detection occurred at 280 nm. Results were processed using Empower software version 2002.

SUPPLEMENTAL INFORMATION

Supplemental Information includes five figures and four tables and can be found with this article online at http://dx.doi.org/10.1016/j.molcel.2016.05.016.

REFERENCES

Allhorn, M., Briceño, J.G., Baudino, L., Lood, C., Olsson, M.L., Izui, S., and Collin, M. (2010). The IgG-specific endoglycosidase EndoS inhibits both cellular and complement-mediated autoimmune hemolysis. Blood *115*, 5080–5088.

Arlaud, G.J., Colomb, M.G., and Gagnon, J. (1987). A functional model of the human C1 complex Emergence of a functional model. Immunol. Today *8*, 106–111.

Bleeker, W.K., Lammerts van Bueren, J.J., van Ojik, H.H., Gerritsen, A.F., Pluyter, M., Houtkamp, M., Halk, E., Goldstein, J., Schuurman, J., van Dijk, M.A., et al. (2004). Dual mode of action of a human anti-epidermal growth factor receptor monoclonal antibody for cancer therapy. J. Immunol. *173*, 4699–4707.

Boyd, P.N., Lines, A.C., and Patel, A.K. (1995). The effect of the removal of sialic acid, galactose and total carbohydrate on the functional activity of Campath-1H. Mol. Immunol. *32*, 1311–1318.

Brier, S., Pflieger, D., Le Mignon, M., Bally, I., Gaboriaud, C., Arlaud, G.J., and Daniel, R. (2010). Mapping surface accessibility of the C1r/C1s tetramer by chemical modification and mass spectrometry provides new insights into assembly of the human C1 complex. J. Biol. Chem. *285*, 32251–32263.

Burton, D.R. (1986). Is IgM-like dislocation a common feature of antibody function? Immunol. Today *7*, 165–167.

Burton, D.R. (1990). Antibody: the flexible adaptor molecule. Trends Biochem. Sci. *15*, 64–69.

Burton, D.R., Pyati, J., Koduri, R., Sharp, S.J., Thornton, G.B., Parren, P.W., Sawyer, L.S., Hendry, R.M., Dunlop, N., Nara, P.L., et al. (1994). Efficient neutralization of primary isolates of HIV-1 by a recombinant human monoclonal antibody. Science *266*, 1024–1027.

Cooper, N.R. (1985). The classical complement pathway: activation and regulation of the first complement component. Adv. Immunol. *37*, 151–216.

Czajkowsky, D.M., and Shao, Z. (2009). The human IgM pentamer is a mushroom-shaped molecule with a flexural bias. Proc. Natl. Acad. Sci. USA *106*, 14960–14965.

de Jong, R.N., Beurskens, F.J., Verploegen, S., Strumane, K., van Kampen, M.D., Voorhorst, M., Horstman, W., Engelberts, P.J., Oostindie, S.C., Wang, G., et al. (2016). A novel platform for the potentiation of therapeutic antibodies based on antigen-dependent formation of IgG hexamers at the cell surface. PLoS Biol. *14*, e1002344.

de Weers, M., Tai, Y.T., van der Veer, M.S., Bakker, J.M., Vink, T., Jacobs, D.C., Oomen, L.A., Peipp, M., Valerius, T., Slootstra, J.W., et al. (2011). Daratumumab, a novel therapeutic human CD38 monoclonal antibody, induces killing of multiple myeloma and other hematological tumors. J. Immunol. *186*, 1840–1848.

Diebolder, C.A., Beurskens, F.J., de Jong, R.N., Koning, R.I., Strumane, K., Lindorfer, M.A., Voorhorst, M., Ugurlar, D., Rosati, S., Heck, A.J.R., et al. (2014). Complement is activated by IgG hexamers assembled at the cell surface. Science *343*, 1260–1263.

Duncan, A.R., and Winter, G. (1988). The binding site for C1q on IgG. Nature *332*, 738–740.

Dyachenko, A., Wang, G., Belov, M., Makarov, A., de Jong, R.N., van den Bremer, E.T.J., Parren, P.W., and Heck, A.J.R. (2015). Tandem native mass-spectrometry on antibody-drug conjugates and submillion Da antibody-antigen protein assemblies on an Orbitrap EMR equipped with a high-mass quadrupole mass selector. Anal. Chem. *87*, 6095–6102.

Ehrnthaller, C., Ignatius, A., Gebhard, F., and Huber-Lang, M. (2011). New insights of an old defense system: structure, function, and clinical relevance of the complement system. Mol. Med. *17*, 317–329.

Feinstein, A., Richardson, N., and Taussig, M.I. (1986). Immunoglobulin flexibility in complement activation. Immunol. Today *7*, 169–174.

Gaboriaud, C., Thielens, N.M., Gregory, L.A., Rossi, V., Fontecilla-Camps, J.C., and Arlaud, G.J. (2004). Structure and activation of the C1 complex of complement: unraveling the puzzle. Trends Immunol. *25*, 368–373.

Gaboriaud, C., Ling, W.L., Thielens, N.M., Bally, I., and Rossi, V. (2014). Deciphering the fine details of c1 assembly and activation mechanisms: "mission impossible"? Front. Immunol. *5*, 565.

Goodfellow, J.J., Baruah, K., Yamamoto, K., Bonomelli, C., Krishna, B., Harvey, D.J., Crispin, M., Scanlan, C.N., and Davis, B.G. (2012). An endoglycosidase with alternative glycan specificity allows broadened glycoprotein remodelling. J. Am. Chem. Soc. *134*, 8030–8033.

Halaby, D.M., Poupon, A., and Mornon, J. (1999). The immunoglobulin fold family: sequence analysis and 3D structure comparisons. Protein Eng. *12*, 563–571.

Heck, A.J.R. (2008). Native mass spectrometry: a bridge between interactomics and structural biology. Nat. Methods *5*, 927–933.

Hodoniczky, J., Zheng, Y.Z., and James, D.C. (2005). Control of recombinant monoclonal antibody effector functions by Fc N-glycan remodeling in vitro. Biotechnol. Prog. *21*, 1644–1652.

Hughes-Jones, N.C., and Gardner, B. (1979). Reaction between the isolated globular sub-units of the complement component C1q and IgG-complexes. Mol. Immunol. *16*, 697–701.

Jefferis, R. (2012). Isotype and glycoform selection for antibody therapeutics. Arch. Biochem. Biophys. *526*, 159–166.

Kishore, U., and Reid, K.B. (2000). C1q: structure, function, and receptors. Immunopharmacology *49*, 159–170.

Kojouharova, M., Reid, K., and Gadjeva, M. (2010). New insights into the molecular mechanisms of classical complement activation. Mol. Immunol. *47*, 2154–2160.

Krapp, S., Mimura, Y., Jefferis, R., Huber, R., and Sondermann, P. (2003). Structural analysis of human IgG-Fc glycoforms reveals a correlation between glycosylation and structural integrity. J. Mol. Biol. *325*, 979–989.

Kuznetsov, Y.G., Day, J., Newman, R., and McPherson, A. (2000). Chimeric human-simian anti-CD4 antibodies form crystalline high symmetry particles. J. Struct. Biol. *131*, 108–115.

Labrijn, A.F., Meesters, J.I., Priem, P., de Jong, R.N., van den Bremer, E.T.J., van Kampen, M.D., Gerritsen, A.F., Schuurman, J., and Parren, P.W. (2014). Controlled Fab-arm exchange for the generation of stable bispecific IgG1. Nat. Protoc. *9*, 2450–2463.

Leatherbarrow, R.J., Rademacher, T.W., Dwek, R.A., Woof, J.M., Clark, A., Burton, D.R., Richardson, N., and Feinstein, A. (1985). Effector functions of a monoclonal aglycosylated mouse IgG2a: binding and activation of complement component C1 and interaction with human monocyte Fc receptor. Mol. Immunol. *22*, 407–415.

Lund, J., Takahashi, N., Pound, J.D., Goodall, M., and Jefferis, R. (1996). Multiple interactions of IgG with its core oligosaccharide can modulate recognition by complement and human Fc gamma receptor I and influence the synthesis of its oligosaccharide chains. J. Immunol. *157*, 4963–4969.

Pawluczkowycz, A.W., Beurskens, F.J., Beum, P.V., Lindorfer, M.A., van de Winkel, J.G., Parren, P.W., and Taylor, R.P. (2009). Binding of submaximal C1q promotes complement-dependent cytotoxicity (CDC) of B cells opsonized with anti-CD20 mAbs ofatumumab (OFA) or rituximab (RTX): considerably higher levels of CDC are induced by OFA than by RTX. J. Immunol. *183*, 749–758.

Petillot, Y., Thibault, P., Thielens, N.M., Rossi, V., Lacroix, M., Coddeville, B., Spik, G., Schumaker, V.N., Gagnon, J., and Arlaud, G.J. (1995). Analysis of the N-linked oligosaccharides of human C1s using electrospray ionisation mass spectrometry. FEBS Lett. *358*, 323–328.

Pflieger, D., Przybylski, C., Gonnet, F., Le Caer, J.P., Lunardi, T., Arlaud, G.J., and Daniel, R. (2010). Analysis of human C1q by combined bottom-up and top-down mass spectrometry: detailed mapping of post-translational

modifications and insights into the C1r/C1s binding sites. Mol. Cell. Proteomics 9, 593–610.

Pinteric, L., Painter, R.H., and Connell, G.E. (1971). Ultrastructure of the Fc fragment of human immunoglobulin G. Immunochemistry 8, 1041–1045.

Reid, K.B.M. (1979). Complete amino acid sequences of the three collagen-like regions present in subcomponent C1q of the first component of human complement. Biochem. J. 179, 367–371.

Saphire, E.O., Parren, P.W.H.I., Pantophlet, R., Zwick, M.B., Morris, G.M., Rudd, P.M., Dwek, R.A., Stanfield, R.L., Burton, D.R., and Wilson, I.A. (2001). Crystal structure of a neutralizing human IGG against HIV-1: a template for vaccine design. Science 293, 1155–1159.

Sledge, C.R., and Bing, D.H. (1973). Binding properties of the human complement protein Clq. J. Biol. Chem. 248, 2818–2823.

Snijder, J., Uetrecht, C., Rose, R.J., Sanchez-Eugenia, R., Marti, G.A., Agirre, J., Guérin, D.M.A., Wuite, G.J.L., Heck, A.J.R., and Roos, W.H. (2013). Probing the biophysical interplay between a viral genome and its capsid. Nat. Chem. 5, 502–509.

Snijder, J., van de Waterbeemd, M., Damoc, E., Denisov, E., Grinfeld, D., Bennett, A., Agbandje-McKenna, M., Makarov, A., and Heck, A.J.R. (2014). Defining the stoichiometry and cargo load of viral and bacterial nanoparticles by Orbitrap mass spectrometry. J. Am. Chem. Soc. 136, 7295–7299.

Strang, C.J., Siegel, R.C., Phillips, M.L., Poon, P.H., and Schumaker, V.N. (1982). Ultrastructure of the first component of human complement: electron microscopy of the crosslinked complex. Proc. Natl. Acad. Sci. USA 79, 586–590.

Tao, M.H., and Morrison, S.L. (1989). Studies of aglycosylated chimeric mouse-human IgG. Role of carbohydrate in the structure and effector func-tions mediated by the human IgG constant region. J. Immunol. 143, 2595–2601.

Teeling, J.L., French, R.R., Cragg, M.S., van den Brakel, J., Pluyter, M., Huang, H., Chan, C., Parren, P.W., Hack, C.E., Dechant, M., et al. (2004). Characterization of new human CD20 monoclonal antibodies with potent cyto-lytic activity against non-Hodgkin lymphomas. Blood 104, 1793–1800.

Tsuchiya, N., Endo, T., Matsuta, K., Yoshinoya, S., Aikawa, T., Kosuge, E., Takeuchi, F., Miyamoto, T., and Kobata, A. (1989). Effects of galactose deple-tion from oligosaccharide chains on immunological activities of human IgG. J. Rheumatol. 16, 285–290.

van den Bremer, E.T.J., Beurskens, F.J., Voorhorst, M., Engelberts, P.J., de Jong, R.N., van der Boom, B.G., Cook, E.M., Lindorfer, M.A., Taylor, R.P., van Berkel, P.H.C., and Parren, P.W. (2015). Human IgG is produced in a pro-form that requires clipping of C-terminal lysines for maximal complement activation. MAbs 7, 672–680.

Wang, G., Johnson, A.J., and Kaltashov, I.A. (2012). Evaluation of electrospray ionization mass spectrometry as a tool for characterization of small soluble protein aggregates. Anal. Chem. 84, 1718–1724.

Yang, R., Otten, M.A., Hellmark, T., Collin, M., Björck, L., Zhao, M.H., Daha, M.R., and Segelmark, M. (2010). Successful treatment of experimental glomer-ulonephritis with IdeS and EndoS, IgG-degrading streptococcal enzymes. Nephrol. Dial. Transplant. 25, 2479–2486.

Zhang, M.X., Bohlman, M.C., Itatani, C., Burton, D.R., Parren, P.W., St Jeor, S.C., and Kozel, T.R. (2006). Human recombinant antimannan immunoglobulin G1 antibody confers resistance to hematogenously disseminated candidiasis in mice. Infect. Immun. 74, 362–369.